

**SEISMIC SHAKING REMOVAL OF CRATERS 0.2 -0.5 KM IN DIAMETER ON ASTEROID 433 EROS.**

P.C. Thomas<sup>1</sup>, M .S. Robinson<sup>2</sup>, <sup>1</sup>Center for Radiophysics and Space Research, Cornell Univ., Ithaca NY 14853, thomas@baritone.astro.cornell.edu, <sup>2</sup>Northwestern Univ., Center for Planetary Sciences, Evanston, IL, 60208,.

Impact cratering acts in a variety of ways to create a surprising range of scenery on small satellites and asteroids. The visible crater population is a self-modifying characteristic of these airless objects, and determining the various ways younger craters can add or subtract from the population is an important aspect of small body "geology." Asteroid 433 Eros, the most closely studied of any small body, has two aspects of its crater population that have attracted attention: a fall-off of crater densities below ~100 m diameter relative to an expected equilibrium population [1] and regions of substantially lower large crater densities [2, 3, 4].

In this work we examine the global variation of the density of craters on Eros larger than 0.177 km, a size range above that involved in small crater depletion hypotheses [1, 5]. We counted all craters on Eros to a size range somewhat below 0.177 km diameter (and different from data used in [3]). The primary metric for this study is the number of craters between 0.177 and 1.0 km within a set radius of each grid point on the 2° x 2° shape model of Eros. This number can be expressed as an R-value [6], provided that it is remembered that the large bin size makes individual R values slightly different from those obtained in the usual root-2 bins.

A sampling radius of 2 km was found to include 0 to 50 craters of this size range; R values range from 0 to 0.36 (again, slightly higher than for the smaller bin size), with the mode at 0.18. Values below 0.14 are in the 7.6 km diameter crater Shoemaker (IAU: Charlois Regio), 10 km diameter Himeros, and 5.4 km diameter Psyche, areas south of Himeros surrounding the rim of Shoemaker, and extending southeast and northeast from Psyche. The transition from low to high crater density can be seen in some individual MSI images (Fig. 1).

The low crater density inside the large three craters has been cited as due to younger ages and possibly effects of high slopes [2, 3], with Shoemaker having the lowest density of craters, confirmed in our counts. The extended area of low crater density, however, includes low slope areas, and crater density within Shoemaker and Himeros does not always correlate well with slopes.

The low crater density areas might be due to covering by ejecta from the young Shoemaker crater, which is the dominant source of the block population on Eros [7]. However, the pattern of the larger blocks, a proxy for Shoemaker ejecta, as well as

predictions of where Shoemaker ejecta should fall [7], do not match the distribution of low crater densities.

We test whether a simple geometric or geophysical relation exists between the crater density and Shoemaker crater. First, we compare the average R values with straight line distance from the center of Shoemaker (~14°S, 334°W, Fig. 2A, B). We have used the global average R values with 2 km radius of sampling, and 1 km radius sampling confined to the side of Eros with Shoemaker. Within 5 km of the center of Shoemaker (Fig. 2A; crater radius is ~3.8 km) the R values are low; they rise steadily to values between 0.15 and 0.23 at 10-11 km distance, using either mapping set. One of the key features of the distance relationship is that the areas of low crater density east of Psyche, on the other side of Eros from Shoemaker crater, also fall into a distance bin of less than 10.5 km. We also have mapped narrower size ranges: 0.177 km to 0.5 km, and 0.5 km to 2 km (because of the crater distribution, the smaller size craters within these large bins dominate the numbers). The results are shown in Fig. 2B. Here again, the bin width makes direct comparison to standard root 2 bins indirect. These plots show that the effect relative to Shoemaker includes craters 0.5 km in diameter.

Because the data appear more consistent with simple geometry relative to Shoemaker, rather than with ejecta patterns, we make a specific test for possible seismic jolt effects [8]. Here we assume that effects might scale as  $D^{-2}$ , or simply as an energy density on a sphere centered on the impact (the current surface center may not be the perfect position for this). Further scaling is invoked as proportional to local gravity, which varies from 0.24 to 0.56 cm s<sup>-2</sup> on Eros [9]. The logic here is that if material at the surface is disturbed by seismic energy from the impact, the magnitude of disturbance may vary inversely as the local gravity: particles could travel further in lower gravity. This scaling is plotted in Fig. 2C. Because the gravity is very low chiefly in places more than 10 km from Shoemaker, this plot basically confirms the average crater density over much of the surface is dependant upon distance from Shoemaker.

Modeling of seismic effects on asteroids has been tested by comparison to crater density curves for whole objects, or as representative of whole objects [5, 8]. The indication that the impact forming

a 7.6 km crater on Eros effectively removed 0.5 km diameter craters across 10 km distance is similar to the predictions of [8] for asteroids Ida and Gaspra, which bracket the mean size of Eros. The modeling of [5] applies chiefly to the smaller craters.

The detection of an area of specific damage associated with a single cratering event provide one calibration point for effects of large impacts on asteroids.

References: [1] Chapman, C. R. et al. (2002) *Icarus* 155, 104-118. [2] Robinson, M. S. et al. (2002) *Meteoritics and Planet. Sci.* 37, 1651-1684. [3] Berthoud, M. et al. (2001) *Bull. Amer. Astron. Soc.* 33, 1149. [4] Berthoud, M. et al. (2005) *Icarus*, submitted. [5] Richardson, J. E., Melosh, H. J., Greenberg, R. (2004) *Science* 306, 1526-1529. [6] Crater Analysis Technique Working Group (1979) *Icarus* 37, 467-474. [7] Thomas P. C. et al. (2001) *Nature* 413, 394-396. [8] Greenberg, R., et al., (1996) *Icarus* 120, 106-118. [9] Thomas, P. C. et al. (2002) *Icarus* 155, 18-37.

Acknowledgements. Funded in part by Discovery Data Analysis Program. Technical help provided by B. Carcich, K. Consroe, J. Joseph.

Fig. 1. Transition from low crater density (bottom) to higher crater density (top) south of crater Himeros (Center of illuminated surface at 42°S,242°W.). Dulcinea crater seen with high albedo interior halo in lower right is 1.4 km diameter, and is centered at 75°S, 272°W. NEAR image M01494091674.

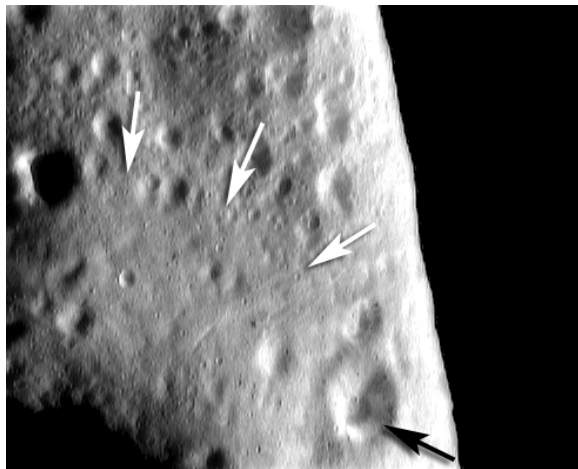


Fig. 2. Crater density metrics in relation to crater Shoemaker. (A) For distance from center of Shoemaker crater to each grid point on shape model, the R value for a sample radius of 2 km, for craters 0.177 – 1.0 km was calculated (sample area larger than grid spacing) (Filled data). Open circles are for 1 km sampling radius, and restricted to 180°-360°W longitudes, the side of Eros with Shoemaker crater. (B) Global 2 km sampled data broken down into smaller width bins. The width of bins affects the calculated R values. Populations of craters of 0.5 km diameter are affected by whatever process is associated with Shoemaker crater. (C) Global data scaled by distance (km) to center of Shoemaker squared, and by local gravity (cm s<sup>-2</sup>). Because gravity varies only modestly within 12 km of Shoemaker, the results are similar to those in A, B.

